JOURNAL OF GEOPHYSICAL RESEARCH, VOL. 101, NO. D17, PAGES 23,021-23,033, OCTOBER 20, 1996

UV-visible absorption cross sections of gaseous Br_2O and HOBr

O.V. Rattigan,[1] D.J. Lary, R.L. Jones, and R.A. Cox

Centre for Atmospheric Science, Department of Chemistry, University of Cambridge, Cambridge, England

Abstract. The absorption cross-section of gaseous HOBr was determined over the wavelength range 235 to 430 nm with a spectral resolution of 0.6 nm full width at half maximum (FWHM) using a diode array spectrometer. The spectrum of HOBr shows two main absorption bands with maxima near 282 nm (σ=(3.1 ± 0.4)x10^{-19} cm^2 $molecule^{-1}$ and 350 nm (σ=12.5 ± 1.6)x10^{-20} cm^2 $molecule^{-1}$) extending out to 430 nm. The absorption cross-sections in the first absorption band are in good agreement with a recent determination; the cross-sections in the second band however, are approximately a factor of 2.5 larger than previously determined. In addition we provide evidence in support of a weak band in HOBr around 440 nm ($\sigma\approx$7.5x10^{-21} cm^2 $molecule^{-1}$) as observed by *Barnes et al.* [1996]. The absorption cross-section of Br_2O, which was used to prepare HOBr, was determined over the wavelength range 230 to 750 nm. The spectrum shows four absorption bands with maxima at 314 nm (σ=(2.1 ± 0.3)x10^{-18} cm^2 $molecule^{-1}$), 350 nm (σ=(1.9 ± 0.2)x10^{-18} cm^2 $molecule^{-1}$), 520 nm (σ=(4.4 ± 0.5)x10^{-20} cm^2 $molecule^{-1}$), and 665 nm (σ=(6.2 ± 0.9)x10^{-20} cm^2 $molecule^{-1}$). The visible bands at 520 nm and 660 nm have not been observed previously. The equilibrium constant, for the reaction $Br_2O + H_2O \Longleftrightarrow 2HOBr$ was determined to be 0.037 ± 0.004 at 298 K. Measurement of the equilibrium constant as a function of temperature enabled values for $\Delta H_{298\ K}$ = (13.0 ± 0.5) kJ mol^{-1} and $\Delta S_{298\ K}$ = (16 ± 2) J mol^{-1} K^{-1} to be determined. The absorption cross-section data for HOBr have been used in a photochemical box model to investigate the significance of these results in the lower stratosphere. The model results are compared with observations during a recent Stratospheric Photochemistry, Aerosols and Dynamics Expedition (SPADE) and show that the revised HOBr cross-section, coupled to the rapid heterogeneous conversion of $BrONO_2$ to HOBr, can account quantitatively for the abrupt morning rise in HO_x.

Introduction

Interest in the spectroscopy of atmospheric bromine species has been stimulated by their role as catalysts in stratospheric ozone depletion [*Yung et al.*, 1980]. HOBr is thought to be a major bromine reservoir produced by the gas phase reaction of BrO with HO_2 (*Poulet et al.* [1992], *Bridier et al.* [1993]):

(R1) $HO_2 + BrO \longrightarrow HOBr + O_2$

and by the hydrolysis of $BrONO_2$ which occurs heterogeneously on atmospheric aerosol particles (*Hanson and Ravishankara* [1995], *Lary et al.* [1996]):

(R2) $H_2O + BrONO_2 \longrightarrow HOBr + HNO_3$

Reaction (R2) followed by the photolysis of HOBr has recently been suggested as a possible source of OH radicals in the lower stratosphere (*Hanson and Ravishankara* [1995]).

The heterogeneous reaction between HOBr and HCl which links the Cl and Br cycles is also thought to be important particularly in polar regions (*Abbatt* [1994]):

(R3) $HOBr + HCl \longrightarrow BrCl + H_2O$

At midlatitudes however, the following O_3 destruction catalytic cycle can occur (*Yung et al.* [1980], *Garcia and Solomon* [1994]), starting with (R1):

(R1) $HO_2 + BrO \longrightarrow HOBr + O_2$
(R4) $HOBr + h\nu \longrightarrow OH + Br$
(R5) $OH + O_3 \longrightarrow HO_2 + O_2$
(R6) $Br + O_3 \longrightarrow BrO + O_2$
Net: $2O_3 \longrightarrow 3O_2$

[1]Now at Department of Chemistry, Boston College, Chestnut Hill, Boston, Massachusetts.

Paper number 96JD02017.
0148-0227/96/96JD-02017$09.00

At altitudes >30 km HOBr can also be destroyed via the reaction with $O(^3P)$ (*Nesbitt et al.* [1995]).

(R7) $HOBr + O(^3P) \longrightarrow BrO + OH$

However, despite the importance of HOBr in the atmosphere, information on the UV visible absorption spectrum is rather limited. The first determination of the UV-visible absorption cross-section of gaseous HOBr has been made only recently by *Orlando and Burkholder* [1995]. As part of a study of bromine oxides we have redetermined the UV visible absorption cross-sections for gaseous HOBr and Br_2O. The results are compared with the recent measurements of *Orlando and Burkholder* [1995].

The measured cross-sections for HOBr have been used to calculate j_{HOBr} in a photochemical box model which includes heterogeneous bromine chemistry to assess its potential for OH production in the lower stratosphere as suggested by *Hanson and Ravishankara* [1995]. The model results are compared to recent observations of *Salawitch et al.* [1994].

Experimental Method

Apparatus

The experimental system consisted of a double-jacketed quartz cell, 100 cm long x 2.0 cm diameter, which was coupled to a dual-beam diode array spectrometer (*Rattigan et al.* [1993]). Two different gratings were used for the spectral measurements. A 150 grooves per mm grating with a spectral range of $\approx$ 305 nm dispersed over a 512 element array was used for spectral measurements of Br_2O in the wavelength region 460 to 750 nm and for HOBr in the wavelength range 263 to 569 nm. In all other cases a 600 grooves per mm grating with a spectral range of $\approx$ 75 nm was used. An entrance slit width of 100 μm was used in both cases providing resolutions of $\approx$ 2.5 nm (FWHM) and 0.6 nm full width half maximum (FWHM) respectively. The higher resolution of the 600 groove per mm grating greatly aided in the spectral subtraction of Br_2 and Br_2O. With this grating measurements were made over several different spectral regions from 235 to 590 nm, ensuring a 10 to 15 nm overlap between adjacent segments. For measurements at wavelengths >300 nm a Pyrex filter was mounted in the monitoring beam to avoid higher order radiation from reaching the detector. For the Br_2O spectrum a filter with a cutoff at 420 nm was used in the spectral measurements of the band from 550 to 750 nm. Wavelength calibrations were made using emission lines of Hg, Zn and Cd from a Philips 93145 spectral lamp and an entrance slit width of 10 μm. The accuracy of the wavelength calibrations are 0.6 nm for the 150 groove per mm grating and 0.15 nm for the 600 groove per mm grating. Gas pressures were measured on a calibrated 100 torr Baratron capacitance manometer (MKS Instruments).

Sample Preparation

HOBr was prepared by the addition of H_2O vapor to a sample of Br_2O in the absorption cell and allowing the establishment of the following equilibrium

(R8) $Br_2O + H_2O \Longleftrightarrow 2HOBr$

Thus from the change in Br_2O upon addition of excess H_2O it was possible to determine the HOBr concentration. Since this method relies on an accurate knowledge of the Br_2O concentration, it was therefore necessary to first prepare Br_2O and measure its absorption cross section in the absence of H_2O vapor.

Br_2O was prepared by the reaction of gaseous Br_2 (Aristar grade 99.95%, BDH Ltd.) with dry yellow HgO powder (99%, Aldrich) as described by *Zintl and Rienäcker* [1930]:

(R9) $2Br_2 + HgO \longrightarrow Br_2O + HgBr_2$

Approximately 60 torr of Br_2 was frozen onto 3 to 4 g of HgO in a trap at 77 K. The trap was then warmed to 263 K over a period of 30 to 60 mins after which the contents were frozen into a second trap at 77 K located close to the absorption cell. Since reaction (R9) was found to yield at most 1-2% Br_2O it was necessary to concentrate the sample by repeating the above procedure four to five times to ensure sufficient Br_2O for spectral measurements. Careful distillation of the second trap contents over a period of several hours at 213 K resulted in a small amount of red/brown material which was typically 70-80% Br_2O, the remainder being Br_2. The sample of Br_2O obtained from this method was sufficient for three to four experiments. For spectral measurements the trap at 213 K was allowed to warm up to room temperature and a sample of Br_2O was measured into the absorption cell. In between measurements the sample of Br_2O was kept in a darkened trap at 213 K.

Results

Absorption Spectrum of Br_2O

In all cases samples of Br_2O contained considerable amounts of Br_2. Furthermore, samples of Br_2O in the absorption cell were found to undergo thermal decomposition into molecular Br_2. In order to determine the spectrum of Br_2O, it was necessary to quantitatively subtract the absorption due to Br_2 using a reference spectrum of Br_2 recorded with the same spectral resolution. Br_2 shows vibrational structure in its absorption spectrum in the region from 515 to 565 nm due to the electronic transition $B^3\Pi(O_u^+) \longleftarrow X^1\Sigma_g^+$. Quantitative subtraction of the Br_2 absorption present in each sample was carried out using a least squares fit to the differential spectra of the sample containing Br_2O and Br_2 and the Br_2 reference over this structured region.

A typical fit is shown in figure 1 at 298 K. Figure 2 shows a sample Br_2O/Br_2 spectrum (line a), estimated Br_2 (0.02 torr) in the sample using the fitting routine (line b) and the residual spectrum (Br_2O = 0.07 torr) (line c) after spectral subtraction of (line b) from (line a) in the region 490 to 565 nm.

The amount of Br_2O present in each sample was estimated by converting the Br_2O into Br_2 by photolysis. Absorption cross sections for Br_2 of *Seery and Britton* [1964] were used to determine the amount of Br_2 present in the samples before and after photolysis and the Br_2O concentration was determined by difference. Small amounts of BrO $\approx$ 1-2 x 10^{12} molecule cm^{-3} were detected during the illumination period consistent with conversion by the following reaction mechanism as proposed by *Orlando and Burkholder* [1995]:

(R10) $Br_2O + h\nu \longrightarrow Br + BrO$
(R11) $Br + Br_2O \longrightarrow Br_2 + BrO$
(R12) $BrO + BrO \longrightarrow 2Br + O_2$
(R13) $BrO + BrO \longrightarrow Br_2 + O_2$

The above mechanism results in the following overall stoichiometric reaction:

$$2\ Br_2O \longrightarrow 2\ Br_2 + O_2$$

From a knowledge of the Br_2O concentration and the absorption spectrum, the absorption cross-sections for Br_2O could then be determined using the Beer Lambert Law. A complete spectrum for Br_2O was subsequently constructed from 240 to 750 nm by recording spectra in several regions working towards shorter wavelengths and ensuring an overlap of at least 15 nm between adjacent segments. Correction for the contribution due to Br_2 at shorter wavelengths was carried out from a knowledge of the spectral shape and the absorption cross-sections of Br_2O and Br_2 in the overlap region.

Figure 3 shows the cross-sections of Br_2O determined by the above described method, compared to the recent

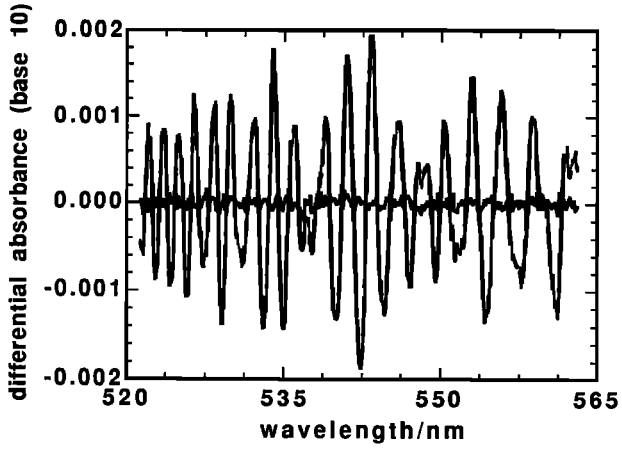

Figure 1. Differential fit of a sample spectrum containing Br_2O + Br_2 (dashed line) to the Br_2 reference spectrum (solid line) and the residuals after subtraction (thick line). Instrument resolution is 0.6 nm (FWHM).

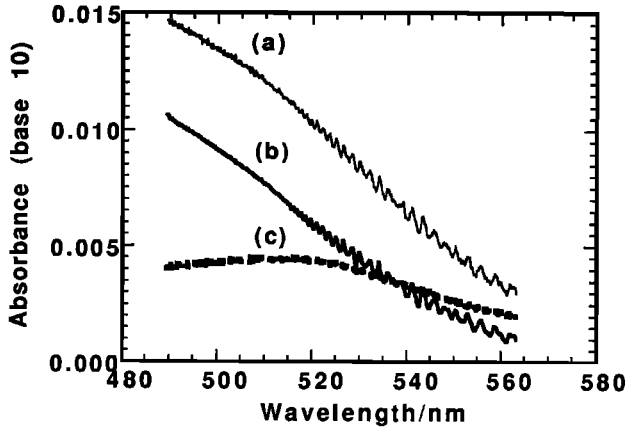

Figure 2. Sample spectrum containing approximately 0.1 torr of Br_2O + Br_2 (line a), Br_2 reference spectrum (line b) and the Br_2O spectrum (line c) after subtraction of (line b) from (line a). Instrument resolution is 0.6 nm (FWHM).

values reported by *Orlando and Burkholder* [1995]. Tabulated values are given in Table 1. There is very good agreement (to within $\approx$ 10%) between the two studies at wavelengths shorter than 400 nm. The absorption cross section at the maximum near 314 nm = (2.1 $\pm$ 0.3)x10^{-18} cm^2 $molecule^{-1}$ is in good agreement with the earlier value of (2.3 $\pm$ 0.3)x10^{-18} cm^2 $molecule^{-1}$. However, at wavelengths greater than 400 nm the values from this study are significantly higher than those of *Orlando and Burkholder* which show a cutoff at $\approx$ 440 nm. The difference between the two measurements is approximately an order of magnitude at 430 nm. *Orlando and Burkholder* used a shorter path length cell of 20 cm and their observed residuals after subtraction of Br_2 from their spectra were $\approx$ 5x10^{-4} (at the detection limit) at wavelengths greater than 440 nm. In the subtraction of Br_2 from their samples of Br_2O they assumed that the absorbance due to Br_2O was zero at 440 nm and beyond. In the present experiments (path length $\approx$ 100 cm) the procedure used to correct for Br_2

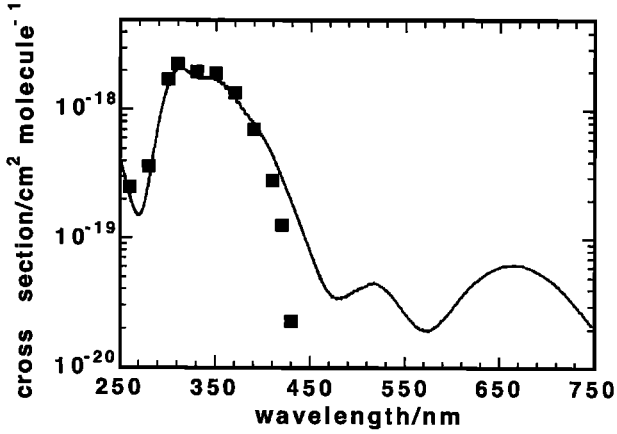

Figure 3. Absorption cross-sections of Br_2O at 298 K determined in this work (solid line) and selected data of *Orlando and Burkholder* [1995] (squares).

Table 1. Absorption cross-sections of Br_2O and HOBr at 298 K

Wavelength (nm)	Br_2O (10^{-18} cm^2 molecule^{-1})		HOBr (10^{-20} cm^2 molecule^{-1})	
	Orlando & Burkholder [1995]	This Work	*Orlando & Burkholder* [1995]	This Work
240	0.869	0.805	0.43	6.68
245	0.630	0.601	1.88	5.22
250	0.443	0.429	4.53	6.74
255	0.322	0.303	8.24	9.93
260	0.249	0.218	12.9	14.1
265	0.211	0.169	18.5	18.9
270	0.206	0.152	24.0	23.9
275	0.252	0.182	28.5	28.0
280	0.361	0.279	30.8	30.4
285	0.571	0.470	30.4	30.8
290	0.883	0.770	27.3	28.7
295	1.30	1.16	22.3	25.2
300	1.72	1.55	16.4	20.9
305	2.07	1.86	10.5	16.8
310	2.26	2.04	7.02	13.8
315	2.29	2.08	4.78	11.8
320	2.20	1.95	3.95	10.8
325	2.08	1.87	4.19	10.6
330	1.99	1.78	4.89	11.0
335	1.94	1.74	5.34	11.5
340	1.94	1.74	5.69	12.0
345	1.94	1.74	5.98	12.3
350	1.91	1.71	5.98	12.5
355	1.82	1.64	5.89	12.2
360	1.64	1.53	5.70	11.6
365	1.51	1.38	5.22	10.7
370	1.36	1.23	4.53	9.59
375	1.15	1.09	3.81	8.37
380	0.988	0.971	3.02	7.40
385	0.835	0.868	2.25	6.22
390	0.704	0.776	1.67	5.08
395	0.600	0.689	1.08	4.13
400	0.487	0.603	0.18	3.27
405	0.382	0.519	0.29	2.56
410	0.283	0.439	0.0	2.04
415	0.201	0.365		1.59
420	0.126	0.298		1.28
425	0.070	0.241		1.06
430	0.023	0.194		0.92
435		0.155		0.84
440		0.123		0.74
445		0.099		0.71
450		0.079		0.67
455		0.063		0.65
460		0.051		0.61
465		0.044		0.53
470		0.038		0.49
475		0.035		0.40
480		0.035		0.34
485		0.035		0.28
490		0.036		0.21
495		0.038		0.14
500		0.040		0.09
505		0.042		0.05
510		0.043		0.0
515		0.045		

was by fitting to the vibrational structure in the Br_2 spectrum referred to above and appreciable absorption which was not due to Br_2 was observed at wavelengths >440 nm as shown in figure 2. The residuals obtained after spectral subtraction using the differential method were typically $\approx \pm 1 \times 10^{-4}$, showing no systematic variation over an approximate order of magnitude range in Br_2 concentration. Two further bands were observed in the visible region of the spectrum; the first one peaking around 520 nm with a cross-section of $\approx 4 \times 10^{-20}$ cm^2

molecule^{-1} and a second broader band from 580 nm extending beyond 750 nm with a peak cross-section of 6.2 x 10^{-20} cm^2 molecule^{-1} at 665 nm. These bands can with reasonable confidence be assigned to Br_2O since similar bands have also been observed in the chlorine analogue, Cl_2O, at 420 and 540 nm, albeit with cross-sections somewhat lower. The spectrum of Br_2O reported here is in good agreement with an earlier reported spectrum obtained during the decomposition of OBrO (*Rattigan et al.* [1994]). The Br_2O spectrum, unlike that of Cl_2O exhibits a vibrational band progression in the wavelength region 345 to 390 nm; the vibrational spacing being $\approx$ 300 cm^{-1}.

Absorption Spectrum of HOBr

HOBr was prepared by the addition of excess H_2O vapor to samples of Br_2O (prepared by the above method) and allowing equilibrium (R8) to be established. A sample of Br_2O (0.20 torr which contained approximately 30% Br_2) was first measured into the absorption cell and a spectrum was recorded over the wavelength range 355 to 430 nm. Upon addition of water vapor ($\approx$ 9 torr) a dramatic change to the spectrum of the mixture was observed as seen in figure 4. The amount of Br_2O present in the sample was quantified by fitting to its vibrational structure in the differential spectrum as shown in figure 5. The remaining spectrum after subtraction of Br_2O was smooth and showed a large contribution due to Br_2 as well as HOBr (see figure 6). A scaled subtraction of the Br_2 was carried out assuming that HOBr does not contribute significantly at wavelengths greater than 430 nm, using a reference spectrum for Br_2 recorded under the same experimental conditions. This method had to be used because the spectral range did not cover regions where structured absorption occurs both for Br_2O ($\lambda <$ 390 nm) and Br_2 ($\lambda >$ 515 nm). Spectra were recorded over several minutes following the addition of water to the cell. In all cases the residual spectra assigned to HOBr in the wavelength range 355-430 nm were found

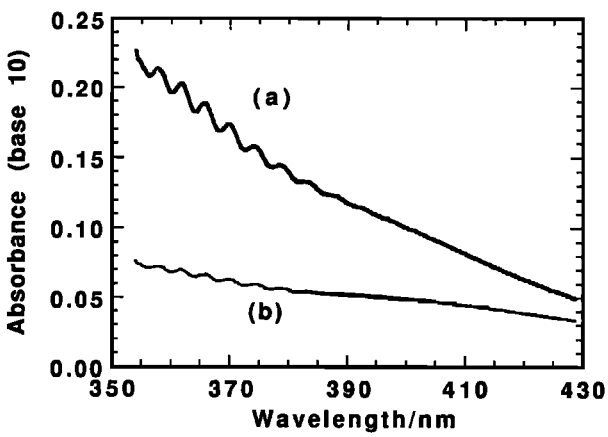

Figure 4. Typical absorption spectrum of a 0.2 torr sample of Br_2O containing 30% Br_2 at 298 K (line a) and the absorption spectrum after the addition of 9 torr of H_2O vapor (line b) to the sample in line a.

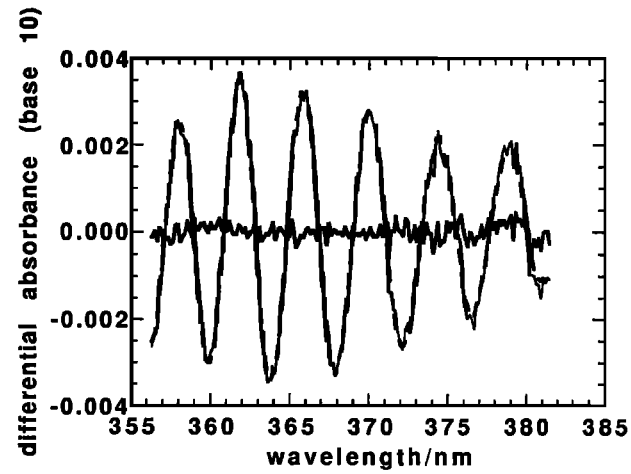

Figure 5. Differential fitting of a sample spectrum containing 0.2 torr Br_2O + Br_2 with 9 torr of H_2O vapor added (solid line) to the Br_2O reference spectrum (dashed line) and the residuals after subtraction (thick dotted line) at 298 K.

to have similar spectral shapes. Furthermore, experiments with a factor of 6 variation in H_2O vapor concentration were carried out in the same wavelength region, and in all cases there was no systematic change to the shape of the HOBr absorption.

In order to provide complete coverage over the wavelength range 235 to 430 nm experiments were carried out at various other spectral regions, working toward shorter wavelengths and ensuring an overlap between adjacent segments of at least 15 nm. Wherever possible, spectral stripping of the Br_2O was carried out using its vibrational structure as discussed above, except in the region 235 to 310 nm where a scaled subtraction was employed. Quantitative subtraction of Br_2 at shorter wavelengths was carried out from a knowledge of the spectral shape of HOBr in the overlap region. In the

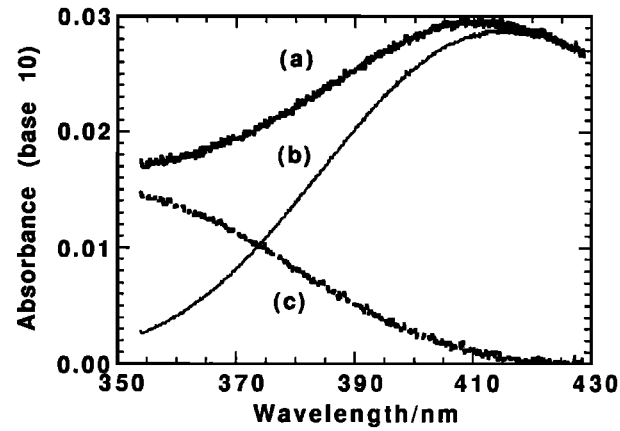

Figure 6. Typical absorption spectrum after the differential subtraction of the contribution due to Br_2O from the $Br_2O/Br_2/H_2O$ spectrum in Figure 4, (line a), a scaled Br_2 reference spectrum (line b) and the residual spectrum assigned to HOBr (line c) after subtraction of line b from line a. See text for details.

wavelength region 235 to 310 nm, however, the correction for Br_2 was negligible and the subtraction of Br_2O was facilitated from a knowledge of the spectral shape of the HOBr at longer wavelengths.

After submission of this work for publication we learned of a new study which employed laser photofragment spectroscopy to determine the relative yields of hydroxyl radicals produced by laser photolysis of mixtures containing Br_2, Br_2O, H_2O and HOBr in the region 440 to 650 nm (*Barnes et al.* [1996]). This work indicates the presence of a weak absorption band for HOBr centered at $\approx$ 440 nm. It is suggested that the band arises from excitation to a triplet state of HOBr. This result implies that the above assumption of zero contribution of HOBr to the composite spectrum at 430 nm is incorrect. In order to investigate the presence of this weak band, we have analyzed spectra of the Br_2O-H_2O-HOBr mixtures taken in our study with the low resolution grating (2.5 nm FWHM) covering the wavelength region 263 to 569 nm. Twenty wideband spectra were analyzed from two mixtures containing initially $4.6x10^{15}$ and $1.8x10^{15}$ molecule cm^{-3} Br_2O with 2.88 torr and 2.45 torr H_2O respectively. After subtraction of the Br_2O absorption using differential fitting to the vibrational structure from 350 to 380 nm as described previously, the Br_2 was subtracted off the remaining spectrum by scaling it to the average absorbance at 435 $\pm$ 5 nm and at 505 $\pm$ 5 nm. The averaged spectra obtained in this way are plotted in figure 10. When zero HOBr contribution at 435 nm was assumed, the spectrum was identical to that obtained in the narrower wavelength region and higher resolution grating (0.6 nm FWHM) and showed a smooth cutoff in absorption in the tail region. However, if zero HOBr absorbance was assumed at 505 nm, a shoulder appeared in the tail, which would be consistent with another weak band centered around 440 nm. Despite having used a Pyrex filter data obtained at wavelengths $>\approx$ 510 nm could not be used because of complications due to second order effects. Time-resolved experiments showed that the absorbance in the shoulder region (430 to 500 nm) varied linearly with that in the band centered around 350 nm, consistent with it being HOBr. The value of the cross-section at 350 nm (σ=$11.5x10^{-20}$ cm^2 $molecule^{-1}$) and the equilibrium constant K_8 (=0.036) obtained from these spectra were close to the average values from all experiments (see below). The absorption at $\lambda < 400$ nm was not significantly changed from the previous high-resolution data.

Absorption Cross section for HOBr

In order to estimate the absorption cross-section for HOBr it is necessary to accurately determine its concentration. This was obtained from estimation of the change in $[Br_2O]$ upon the addition of excess H_2O vapor, which results in the equilibrium (R8) being established (see below):

(R8) $Br_2O + H_2O \iff 2HOBr$

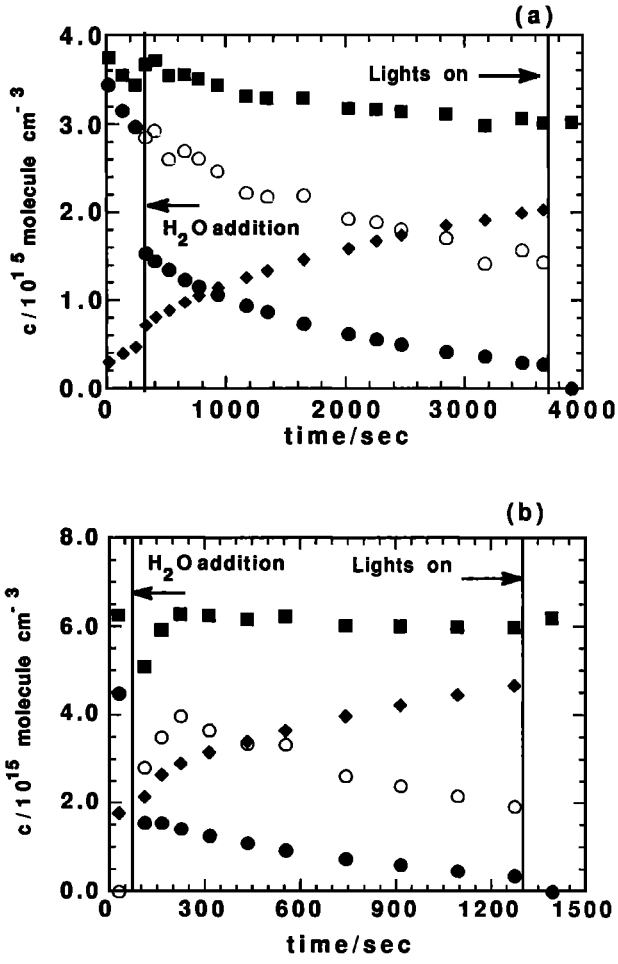

Figure 7. Concentration (10^{15} molecule cm^{-3}) time profile of Br_2O (solid circles), Br_2 (diamonds), HOBr (open circles) and total Br_2 (squares) at 298 K with the addition of (a) 4.3 torr of H_2O and (b) 9.0 torr H_2O to the Br_2O/Br_2 sample. The [HOBr] was estimated from the $\Delta[Br_2O]$ upon addition of the H_2O vapor to the Br_2O/Br_2 sample. See text for details.

The amount of HOBr in the equilibrium mixture was assumed to be given by the stoichiometry:

$$\Delta[HOBr] = 2\Delta[Br_2O] \quad (1)$$

Figure 7(a) shows the concentration-time profile of the various bromine species in the cell when 4.3 torr of H_2O was added to a 0.12 torr sample of Br_2O containing initially $\approx$ 10% Br_2. Prior to the addition of water, Br_2O decayed, with production of Br_2 with a first order decay constant of $(6.6 \pm 1.1)x10^{-4}$ s^{-1}. This is believed to be due to a heterogeneous reaction since the rate was independent of total pressure and tended to decrease in successive experiments as the surface became conditioned. The concentration of Br_2O at the point of H_2O addition was estimated by extrapolation of this decay.

Upon addition of H_2O there was an abrupt drop in the $[Br_2O]$ which then underwent a slow decomposition with concurrent production of Br_2. The slow

loss was first order in $[Br_2O]$ as shown by the semilog plot in figure 8(a), with a decay rate of $(4.91 \pm 0.01)x10^{-4}$ s^{-1}. The $[Br_2O]$ immediately after H_2O addition was obtained by a short back extrapolation, and hence $\Delta[Br_2O]$ could be determined.

After the addition of H_2O the absorption due to HOBr appeared rapidly and then showed a slow first order decay. The slope of the semilog plot (figure 8(b)) was $(2.2 \pm 0.2)x10^{-4}$ s^{-1}, i.e. a factor of 2 less than the slope for Br_2O decay, within the experimental error. This feature was observed in all experiments and provides a strong indication that the equilibrium (R8) was maintained throughout the decay. Back extrapolation of the HOBr absorption to the point of H_2O addition gave the absorption corresponding to $[HOBr] = 2\Delta[Br_2O]$ (see (1)). This was used to calculate σ_{HOBr}, which was then used to compute the values of [HOBr] and total $[Br_2]$ plotted for the remainder of the experiment.

Prior to H_2O addition, $[Br_2O]$ declined while Br_2 increased. However the Br_2 increase was less than the Br_2O loss, as seen from the total Br_2 curve in figure 7(a). Upon addition of H_2O the Br_2 balance was restored and a distinct rapid rise in $[Br_2]$ is evident before the increase due to the slow decomposition of Br_2O and/or HOBr. This behavior was much less apparent at 308 K and is believed to result from the physical adsorption of Br_2 at the vessel walls, with displacement of the adsorbed Br_2 by more strongly absorbed water molecules. In the subsequent period when Br_2 increased, there was a slow loss of total Br_2, which could result from additional surface loss of Br_2.

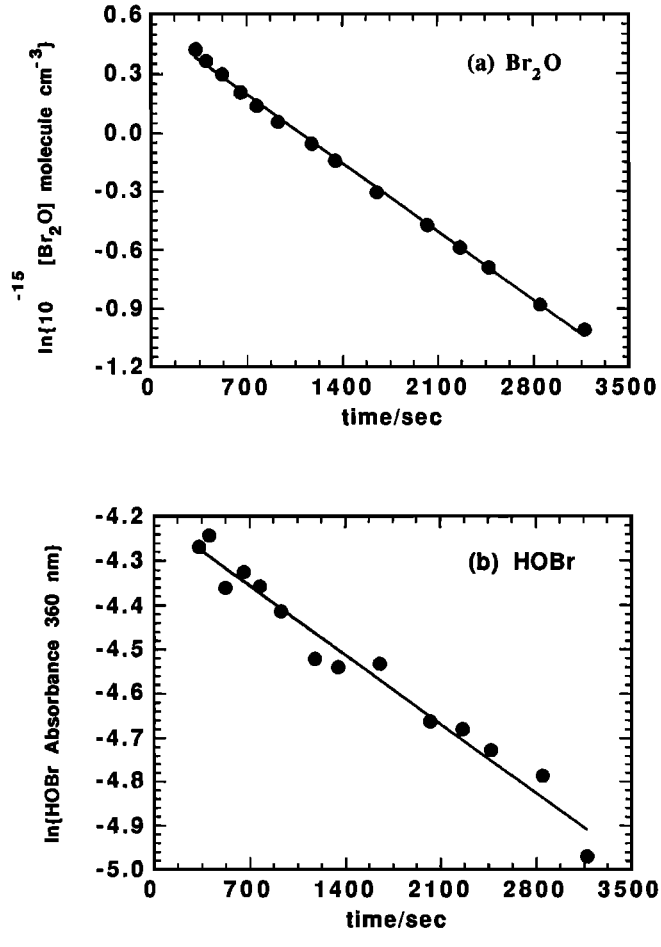

Figure 8. Plots of (a) $\log_e [Br_2O]$ versus time and (b) $\log_e$ HOBr absorbance versus time following the addition of 4.3 torr of H_2O vapor to the Br_2O/Br_2 sample at 298 K. The lines show the least squares fit to the data.

Important differences were observed in experiments with higher added $[H_2O]$ ($P > 8$ torr), an example of which is shown in figure 7(b). After the addition of H_2O there was a distinct delay period before the [HOBr] maximized, while the changes in Br_2 and Br_2O were much less affected. The time period increased with the amount of added H_2O. At first this was thought to be a mixing effect following the addition of a relatively large partial pressure of H_2O to small amounts of Br_2O in the cell. However, when a similar pressure of N_2 was added to the Br_2O/Br_2 mixtures, small perturbations due to mixing could be seen, but they restored on a shorter timescale (<100 s), more in line with diffusive mixing times for these conditions. The slow growth of HOBr is indicative of a surface controlled kinetic effect, probably associated with multilayer adsorption of water, which is likely to occur on a glass surface at relative humidities greater than $\approx$ 40%. During this period the equilibrium between the gaseous Br_2O, H_2O and HOBr was not established and the data could not be used to determine σ or K_8. Beyond this period the HOBr maximized and then decayed with a first order rate of $(6.95 \pm 0.35)x10^{-4}$ s^{-1} i.e. a factor of two lower than that of Br_2O, $(1.29 \pm 0.16)x10^{-3}$ s^{-1}) as also observed at lower $[H_2O]$ in figure 7(a). The 'true' initial HOBr absorption was again determined by back extrapolation to the point of H_2O addition and σ_{HOBr} determined according to (1). There was no systematic variation in σ_{HOBr} determined in this way over a range of $[H_2O]$ as is seen from the data summarized in Table 2.

The second effect of increased $[H_2O]$ was to maintain a better mass balance in total Br_2 during the decay of Br_2O and HOBr. For example, in figure 7(b) following the mixing period the total bromine is reasonably constant as a function of time. Furthermore, the total amount of Br_2 recovered at the end after complete conversion of the HOBr and Br_2O into Br_2 via photolysis, agrees with the initial total concentrations of Br_2O and Br_2, indicating that the estimation of both Br_2O and HOBr are consistent. The better mass balance can be rationalised in terms of the influence of the more strongly adsorbing water molecules, lowering the extent of surface adsorption of Br_2.

Once the HOBr concentration is known, the absorption cross-section can be calculated from the absorbance measurements using the Beer Lambert law. Table 2 shows the values of σ_{HOBr} at 360 nm for a variety of initial conditions at different temperatures in the range

Table 2. Absorption cross-section for HOBr and equilibrium constant K_8 at various temperatures and $[H_2O]$

Temp/K	$[H_2O]$ 10^{-17} molecule cm^{-3}	$\sigma_{360\ nm}$ 10^{20} cm^2 $molecule^{-1}$	K_8[a]
308	3.76	11.0 ± 1.3	0.047 ± 0.003
	2.95	9.56 ± 1.2	0.046 ± 0.002
	1.97	12.3 ± 0.6	0.046 ± 0.002
	1.70	12.8 ± 0.5	0.041± 0.002
	1.45	12.5 ± 0.4	0.043 ± 0.004
	average	11.6 ± 1.2	0.045 ± 0.002
298	4.21	9.84 ± 0.7	0.038 ± 0.003
	3.97	10.9 ± 0.4	0.038 ± 0.004
	3.30	9.26 ± 1.0	0.038 ± 0.003
	3.27	10.9 ± 3.2	0.036 ± 0.004
	2.90	11.2 ± 0.6	0.037 ± 0.003
	2.82	10.4 ± 2.3	0.039 ± 0.003
	1.67	11.7 ± 0.7	0.037 ± 0.002
	1.58	11.7 ± 0.3	0.038 ± 0.002
	1.38	11.4 ± 0.6	0.044 ± 0.006
	0.82	11.2 ± 1.2	0.026 ± 0.003
	0.66	13.6 ± 1.8	0.039 ± 0.007
	0.55	12.2 ± 1.4	0.017 ± 0.003[b]
	average	11.2 ± 1.1	0.037 ± 0.004
288	3.28	11.6 ± 1.1	0.033 ± 0.005
	2.98	12.3 ± 4.5	0.029 ± 0.005
	2.87	13.9 ± 1.6	0.031 ± 0.002
	average	12.6 ± 1.0	0.031 ± 0.002
278	1.736	12.8 ± 1.8	0.028 ± 0.003
	1.371	12.9 ± 0.7	0.028 ± 0.003
	1.041	10.5 ± 1.9	0.023 ± 0.003
	average	12.1 ± 1.1	0.026 ± 0.002

[a] $K_8=[HOBr]^2/[Br_2O][H_2O]$.
[b] not included in the average of K_8

278 to 308 K. There was no significant temperature dependence in the cross-section and the mean value of σ_{360nm} was $(11.6 \pm 1.3)\times10^{-20}$ cm^2 $molecule^{-1}$ (error represents statistical scatter at the 1σ level). As a check on the values of the cross-section determined on the basis of $\Delta[Br_2O]$, the amount of HOBr present immediately after the addition of H_2O was calculated assuming a mass balance of total bromine, i.e.

$$[HOBr]_t = 2x([Br_2O]_i - [Br_2O]_t) - ([Br_2]_t - [Br_2]_i) \quad (2)$$

where i refers to the initial concentrations and t refers to the concentrations at some time after H_2O addition. Because of the delay in the rise in the HOBr absorption (at higher H_2O) and the loss of total bromine at longer reaction times, it was necessary to extrapolate the values of σ calculated from $[HOBr]_t$ to the point of water addition. The mean value of σ_{360nm} calculated in this way was $(9.90 \pm 1.62)\times10^{-20}$ cm^2 $molecule^{-1}$ at 298 K, i.e. 15% lower than the mean value of σ_{360nm} based on $\Delta[Br_2O]$, but within the error limits. The lower value probably arises from an under-estimation of $[Br_2]_t$ due to adsorption of Br_2 at the walls, which will result in an overestimation of [HOBr] calculated by equation (2) and hence lower values for σ_{HOBr}. The higher value given above is therefore preferred.

The absorption cross-sections for HOBr calculated in this study are compared with the previous values of *Orlando and Burkholder* [1995] in figure 9. Tabulated values averaged over 5 nm intervals are shown in Table 1. The uncertainty in the estimation of σ based on the spread of the values is ± 13% at wavelengths <400 nm, increasing rapidly at longer wavelengths due to the assumption made regarding the point where HOBr absorbance becomes negligible compared to the Br_2 impurity. At wavelengths < 300 nm the cross-sections determined here are in good agreement with the previously determined values. The absorption cross-section at the maximum near 282 nm $\sigma=(3.1 \pm 0.4) \times 10^{-19}$ cm^2 $molecule^{-1}$ is in excellent agreement with that obtained by *Orlando and Burkholder*. However, at longer wavelengths which is the most important region for pho-

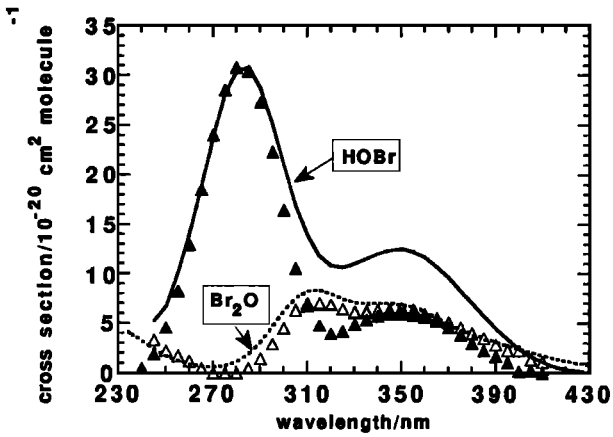

Figure 9. Absorption cross-sections of HOBr at 298 K with a wavelength cutoff at 430 nm determined in this work (solid line) and selected data from *Orlando and Burkholder* [1995] (filled triangles). The difference between this work and that of *Orlando and Burkholder* [1995] is shown by the dashed line. The open triangles show the scaled Br_2O cross-sections determined in this work.

tolysis in the atmosphere, our values are up to a factor of $\approx$ 2.5 higher and significant absorption due to HOBr is measured out to 430 nm. The shape of the HOBr spectrum is very similar to that of the chlorine analogue HOCl, (*Burkholder* [1993]), HOBr being red-shifted by $\approx$ 45 nm. The intensity of the HOBr absorption is however higher than that of HOCl in both bands.

The reason for the discrepancy between our spectrum and that of *Orlando and Burkholder* [1995] at longer wavelengths is immediately apparent when the differences in the cross-section as a function of wavelength are examined, see figure 9. The difference matches well the spectrum of Br_2O, indicating that the discrepancy arises from systematic errors in subtraction of Br_2O in one of the two studies. As seen from figure 5, there is no structure evident in the residual from the least squares fitting routine; a measure of the accuracy in the fitted Br_2O can be determined from the uncertainty in the gradient of a plot of the fitted and the scaled reference spectrum. This was found to be typically better than $\pm$ 2% (2σ) in the present study. However, because the absorption due to Br_2O was an order of magnitude greater than the HOBr absorption at 360 nm, the HOBr cross-sections are quite sensitive to small errors in the amount of Br_2O subtracted. The $\pm$ 2% uncertainty in the Br_2O subtraction translates to $\approx \pm$ 10% error in the HOBr cross-section in the present experiments. Thus the discrepancy in the cross-sections is well outside the error in the present study.

Orlando and Burkholder [1995] also applied differential fitting routines to subtract Br_2O absorption from HOBr, and subtraction of the Br_2 was carried out by a similar method to that used here, i.e. by assuming that only Br_2 absorbed at wavelengths > 440 nm. In the experiments of *Orlando and Burkholder* however the amount of Br_2 was typically $\approx 10^{16}$ molecule cm^{-3}, i.e. approximately an order of magnitude higher than in the present work and the absorption due to Br_2 dominated that of HOBr at wavelengths > 350 nm. This could have lead to uncertainties in the spectral subtraction of Br_2O at longer wavelengths where its structured absorption lies. Thus small errors in the amount of Br_2O would have influenced the derived spectrum and hence the HOBr cross-sections.

During the course of this work we have learned of two further investigations of the absorption spectrum of HOBr. *Benter et al.* [1995] reported cross-section measurements in the region 234 - 400 nm for HOBr, produced by bubbling helium through freshly prepared aqueous 0.2 M HOBr solutions at 293 K. Much lower [Br_2O]/[HOBr] ratios ($\approx$ 0.02 at 293 K) were achieved by this method. HOBr concentrations were determined either by iodometric titration of trapped samples or by gas phase titration of HOBr with Cl atoms in a fast flow system. Spectra were recorded with a photodiode array. The cross-sections reported at the two band maxima were (2.4 $\pm$ 0.1) x 10^{-19} cm^2 molecule^{-1} at 284 nm and 7.7x10^{-20} cm^2 molecule^{-1} at 350 nm. Figure 10 shows a comparison of this and the other HOBr spectra normalized to a value of (3.1 $\pm$ 0.4) x 10^{-19} cm^2 molecule^{-1} at 282 nm. The shape of the *Benter et al.* [1995] spectrum lies closer to the present work than to the *Orlando and Burkholder* [1995] spectrum, but nevertheless the cross-sections are lower in the region of strong Br_2O absorption. Unfortunately, *Benter et al.* [1995] did not extend their measurements beyond 400 nm and they did not discuss their methodology of correction for Br_2O absorption.

In a second study, *Deters et al.* [1996] have presented results from similar experiments to our own, utilising

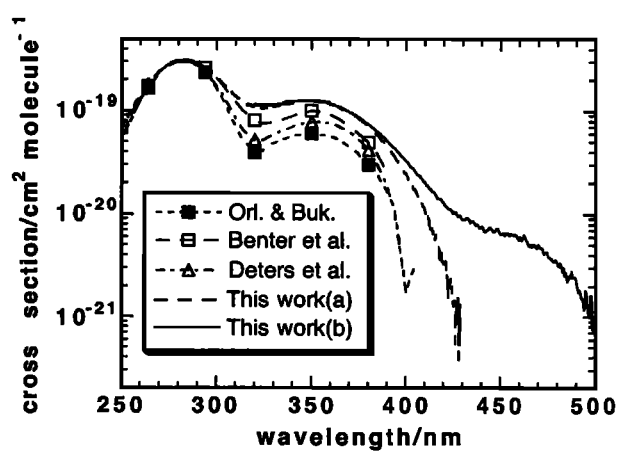

Figure 10. Absorption cross-sections of HOBr determined in this work with a wavelength cutoff at 430 nm (dashed line) and a wavelength cutoff at 510 nm (solid line), *Orlando and Burkholder* (solid squares and dotted line), *Benter et al.* [1995] (open squares and dashed line) and *Deters et al.* [1995] (open triangles and dash-dotted line). Data of *Benter et al.* and *Deters et al.* [1996] are normalized to a value of 3.1 x 10^{-19} cm^2 molecule^{-1} at 282 nm.

the reaction of Br_2O with H_2O to make HOBr. They report cross-sections at the two band maxima of (2.7 ± 0.4)x10^{-19} cm^2 $molecule^{-1}$ at 280 nm and (7.0 ± 1.1)x10^{-20} cm^2 $molecule^{-1}$ at 355 nm. The spectrum normalized at the maximum near 282 nm is also shown in figure 10. It is closer in shape to the *Orlando and Burkholder* [1995] spectrum. Clearly, the differences lie in the subtraction of Br_2O absorption, but details of the methodology for this were not given.

Neither of these studies provides information on the weak absorption band for HOBr centered about 440 nm, detected using photofragment spectroscopy by *Barnes et al.* [1996]. The cross-section at the maximum was estimated by comparing the relative yield of OH, assuming unit quantum yield for dissociation via the process in (R4):

(R4) $HOBr + h\nu \longrightarrow OH + Br$

and utilising the value of σ(355 nm) from *Orlando and Burkholder* [1995]. The value obtained was 8.8x10^{-21} cm^2 $molecule^{-1}$ at 440 nm. If scaled to the present value of 12.5x10^{-20} cm^2 $molecule^{-1}$ at 350 nm the value is 18.0x10^{-21} cm^2 $molecule^{-1}$ at 440 nm which is substantially higher than the cross section obtained from analysis of our wideband spectra, i.e. ≈ 7.5x10^{-21} cm^2 $molecule^{-1}$. Clearly there remains considerable uncertainty about this long wavelength absorption band of HOBr.

Equilibrium Constant $K_8=[HOBr]^2/[Br_2O][H_2O]$

The equilibrium constant for (R8) was determined from the $[Br_2O]$ and [HOBr] present following the addition of a known excess $[H_2O]$. Values for the equilibrium constant K_8 at 298 K as a function of time with an initial H_2O vapor concentration of 2.9x10^{17} molecule cm^{-3} are shown in Table 3. Once mixing is achieved, the values of K_8 are reasonably constant and yield an average value of 0.037 ± 0.003. This value is a factor of ≈ 2 larger than previously determined by *Orlando and Burkholder* [1995]. The value for K_8 remained essentially constant over more than a factor of 6 change in the initial $[H_2O]$ added as shown in Table 2. Furthermore, experiments in different spectral regions did not show any systematic variation in K_8. The average of all the data at 298 K yield a value for K_8 = 0.037 ± 0.004, which is not too dissimilar from the value of (0.1 ± 0.01) for the corresponding equilibrium involving Cl_2O and H_2O [*Burkholder*, 1993].

Experiments have also been conducted at temperatures in the range 278 to 308 K in order to determine the temperature dependence of the equilibrium constant and hence to obtain thermodynamic parameters (ΔH and ΔS) for (R8). For these experiments the spectral region > 290 nm was selected so that accurate subtraction of Br_2O could be carried out using differential fitting to its vibrational fine structure as discussed above. Any temperature dependence in the absorption cross-section of HOBr was assumed to be indistinguishable from the error uncertainties in σ of ± 13% in the limited temperature range used, and was not considered in these calculations. The values obtained for K_8 are shown in Table 2, indicating an approximate factor of 2 change over the experimental temperature range 278 to 308 K. A Van't Hoff plot of ln K_8 versus 1000/T as shown in figure 11 yields a value for ΔH_8 = (13.0 ± 0.5) kJ mol^{-1} and ΔS_8 of about (16 ± 2) J mol^{-1} K^{-1}. This low value for ΔS is expected for the reaction between the triatomic species Br_2O and H_2O forming two triatomic product molecules. The value agrees with the calculated value of ΔS° = 18 J mol^{-1} K^{-1} obtained using *Benson's* [1976] bond additivity method to estimate $S^\circ(Br_2O)_{298\ K}$ = 289 J mol^{-1} K^{-1} and a value for $S^\circ(HOBr)_{298\ K}$ = 248 J mol^{-1} K^{-1} from *McGrath and Rowland* [1994]. Taking an average of the reported val-

Table 3. Equilibrium constant K_8 versus time

Time/sec	K_8[a]	Total $[Br_2]$ x 10^{15} molecule cm^{-3}
30	0	6.254
110	0.018[b]	6.084
164	0.027[b]	5.913
224	0.039	6.280
314	0.036	6.243
434	0.035	6.164
554	0.041	6.234
743	0.032	6.019
914	0.033	5.998
1094	0.035	5.997
1274	0.035	5.970
1394	0.043	6.186
average	0.037 ± 0.003	

Temperature is 298 K; $[H_2O]$ = 2.9x10^{17} molecule cm^{-3}.
[a] $K_8=[HOBr]^2/[Br_2O][H_2O]$.
[b] not included in the average of K_8, see text for details

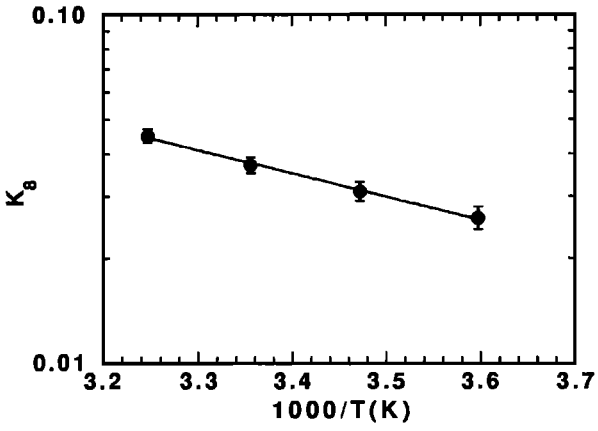

Figure 11. A Van't Hoff plot of $\log_e K_8$ versus 1000/T (K) over the temperature range 273 to 308 K. The line shows the least squares fit to the data. Error bars represent statistical scatter to the data and are expressed as $\pm$ 1σ.

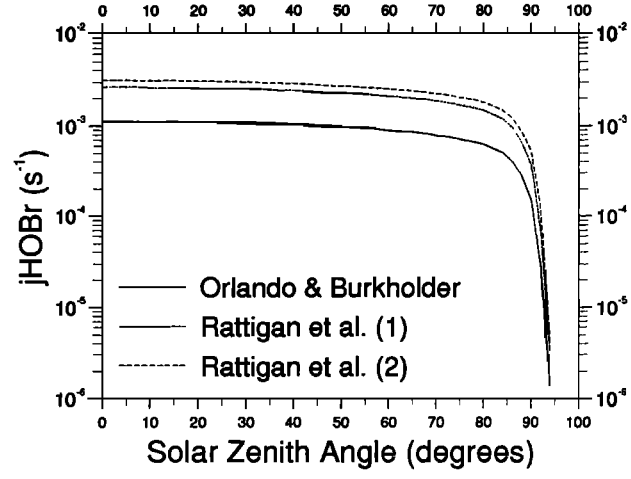

Figure 12. The calculated HOBr photolysis coefficient (s^{-1}) at 70 mbar as a function of solar zenith angle (degrees) using the cross-section data of this study, with a wavelength cut offat 430 nm (dashed line), and a wavelength cutoff at 510 nm (dash-dotted line) and those reported by *Orlando and Burkholder* [1995] (solid line). A midlatitude ozone and temperature profile was used, and a photodecomposition quantum efficiency of unity was assumed.

ues of $\Delta H°(HOBr)_{298\ K}$ = -58.5 kJ mol^{-1} [*McGrath and Rowland*, 1994; *Ruscic and Berkowitz*, 1994; *Glukhovtsev et al.*, 1996; *Lock et al.*, 1996; *Thorn et al.* 1996] and using the above value for ΔH_8, a value for $\Delta H°(Br_2O)$ of 112 kJ mol^{-1} is obtained compared to the recently reported value of 107 kJ mol^{-1} by *Thorn et al.* [1996].

Atmospheric Implications

The absorption cross-sections for HOBr determined in this study have been used in a photochemical box model to calculate the photolysis rate at 70 mbar as a function of solar zenith angle (SZA). For this calculation a midlatitude ozone and temperature profile were used and a photodissociation quantum yield of unity for HOBr was assumed. The calculated photolysis rates (j_{HOBr}) versus SZA are shown in figure 12. As can be seen, the calculated photolysis rate for HOBr is increased by a factor of $\approx$ 2.3 or 2.8, compared with the data of *Orlando and Burkholder* [1995] depending on whether the long wavelength band is included. In the sunlit atmosphere a value of $\approx$ 2.5-3x10^{-3} s^{-1} is obtained, which corresponds to a lifetime for HOBr of $\approx$ 6 minutes indicating that its photodissociation lifetime is comparable to that of $BrONO_2$ [*Lary et al.*, 1996]. The model used accounts for spherical geometry of the atmospheric and all orders of multiple scattering as described by *Lary and Pyle* [1991a,b]. The effect of scattering from clouds however is not considered in these calculations. The model is based on work of *Meier et al.* [1982], *Nicolet et al.* [1982], and *Anderson* [1983].

Recent measurements during the Stratospheric Photochemistry, Aerosols and Dynamics Expedition (SPADE) campaign [*Salawitch et al.*, 1994] indicated a pulse of HO and HO_2 after sunrise at 37.4°N, consistent with the photolysis of a nighttime reservoir of HO_x. An argument was proposed by *Salawitch et al.* [1994], which involved the heterogeneous conversion of HO_2NO_2 into HONO on aerosol particles overnight. The abrupt increase in HO_x at dawn was ascribed to the subsequent photolysis of HONO into OH and NO. However recent measurements by *Zhang et al.* (Heterogeneous chemistry of HO_2NO_2 on liquid sulfuric acid, submitted to *J. Phys. Chem.*, 1995) indicate that the heterogeneous conversion of HO_2NO_2 into HONO is too slow to account for the observed production in HO and HO_2.

The effect of the revised HOBr cross-sections coupled with heterogeneous bromine chemistry on the calculated levels of HO_x has also been investigated. During the night the heterogeneous hydrolysis of $BrONO_2$ on sulphate aerosols produces HOBr [*Hanson and Ravishankara*, 1995] and photolysis of the nighttime accumulated HOBr at sunrise could lead to a rapid rise in OH. As a result little $BrONO_2$ remains if even moderate aerosol loadings are present. *Lary et al.* [1996] have indeed shown that this nighttime production of HOBr leads to a sudden increase in the OH and HO_2 concentrations at dawn, which is similar to those recently reported by *Salawitch et al.* [1994], although the magnitude of this increase was somewhat underestimated in their work. If the HOBr cross-sections reported in this study, however, are used instead of those of *Orlando and Burkholder* [1995], the rate of HOBr photolysis is increased by a factor of $\approx$ 2.5. Figures 13(a) and (b) show that this does not influence greatly the daytime HO_x radical concentrations; it does give a stronger point of inflection in OH and HO_2 at sunrise, which is in better agreement with the SPADE observations than the simulations presented by *Lary et al.* [1996]. In these calculations HOBr cross sections with a cutoff at 430 nm

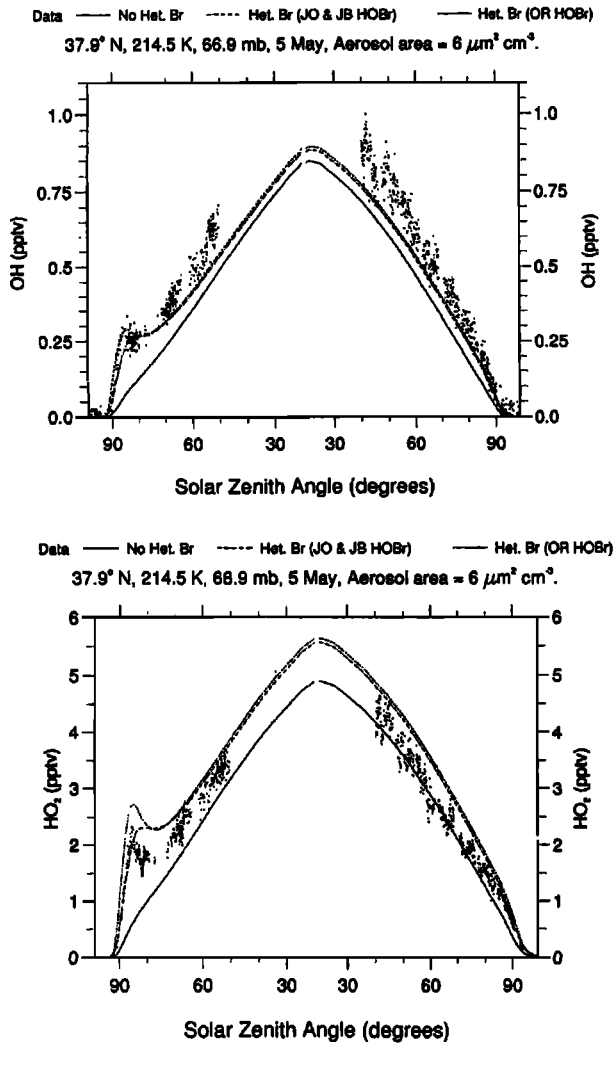

Figure 13. The effect of HOBr photolysis and heterogeneous bromine reactions on sulphate aerosols on the shape of (a) OH and (b) HO_2 diurnal cycles. The initial conditions were taken from Table 1 of *Salawitch et al.* [1994] and an assumed total BrO_y of 11.5 pptv at 66.9 mbar. The solid lines uses the cross-sections of *Orlando and Burkholder* [1995] and does not include heterogeneous bromine chemistry. The dot-dashed line uses the HOBr cross-sections of *Orlando and Burkholder* and includes the heterogeneous bromine reactions as described by *Lary et al.* [1996]. The dashed line uses the HOBr cross-sections determined in this work (wavelength cut-off at 430 nm) and includes heterogeneous bromine reactions as described by *Lary et al.* [1996].

were used (see figure 10). Allowing for the weak band around 440 nm from this work gives a 10-15% earlier risetime in HO and HO_2; the agreement with the 'pulse' in the SPADE data is not greatly affected. If heterogeneous bromine chemistry is not included in the model runs, the model underpredicts the observed HO_x and there is no evidence for an early morning pulse in either OH or HO_2. The simulations shown in figures 13(a) and (b) used the initial conditions given by *Salawitch et al.* [1994, Table 1] and assumed a total BrO_y of 11.5 parts per trillion by volume (pptv) at 66.9 mbar. The model used was AUTOCHEM, described in detail by *Lary et al.* [1996].

The increased photolysis rate of HOBr coupled with the hydrolysis of $BrONO_2$ on the surface of sulphate aerosols causes a 10-20% enhancement in the daytime BrO concentrations calculated by the model. In addition, the enhanced OH concentration causes a slight decrease in the HCl lifetime and hence the HCl/ClO_y ratio in the lower stratosphere. This, in turn, causes additional ClO_x and BrO_x activation, which enhances the effectiveness of the gas phase ClO/BrO cycles. The increase in OH and HO_2 also enhances the HO_2/ClO and HO_2/BrO catalytic cycles. The catalytic hydrolysis of $BrONO_2$ leads to a direct conversion of NO_x ($NO + NO_2$) to HNO_3. For sunlit conditions at midlatitudes this direct conversion to HNO_3 is of comparable magnitude to that caused by the hydrolysis of N_2O_5. However, there is also an indirect enhancement in HNO_3 that occurs owing to the increase in the rate of reaction of OH with NO_2. These mechanisms, all of which act together, lead to enhanced loss of O_3 at all latitudes in the lower stratosphere.

This is of interest since a recent World Meteorological Organization (WMO) assessment [*WMO*, 1992] reported that for the first time there were statistically significant decreases in ozone in all seasons in both the northern and southern Hemispheres at midlatitudes and high latitudes during the 1980s, and that most of this decrease is occurring in the lower stratosphere. Trends derived from ozonesondes by *Logan*, [1994] support of these findings. *Solomon et al.* [1996] showed that when a two-dimensional model is constrained with time varying aerosol observations, the shape of the observed trends in ozone are reproduced but their magnitude is about 50% larger than that which is observed. This paper shows that at least part of this ozone loss is likely to be due to insitu heterogeneous bromine reactions. As the hydrolysis of $BrONO_2$ is not very temperature dependent, it can occur at all latitudes. For a more detailed analysis, see *Lary et al.* [1996].

Conclusions

The absorption cross-sections for HOBr appear to be larger at wavelengths 310 to 430 nm than those previously determined by *Orlando and Burkholder* [1995]. The calculated atmospheric photolysis rate is, correspondingly, a factor of 2.5 faster. Inclusion of heterogeneous hydrolysis of $BrONO_2$ into HOBr on sulphate aerosols together with the faster photolysis rate of HOBr brings the model simulations of the details in the diurnal variation of HO and HO_2 into good agreement with the SPADE observations. In addition, the catalytic hydrolysis of $BrONO_2$ leads to enhanced ozone loss at all latitudes in the lower stratosphere. This loss is mainly due to the elevated levels of HO_x and BrO and the reduction in NO_x which enhances the ClO con-

centration, thereby enhancing O_3 loss by the catalytic cycles ClO/BrO, HO_2/ClO, and HO_2/BrO in the lower stratosphere.

Acknowledgments. We thank D.J. Fish for providing the software for the spectral fitting routines and R.J. Salawitch for providing a copy of the SPADE data. Thanks to Amitabha Sinha and Bernd Deters for providing copies of their manuscripts prior to publication. O.V.R. wishes to thank the United Kingdom Research Council (NERC) for financial support.

References

Abbatt, J.P.D., Heterogeneous reaction of HOBr with HBr and HCl on ice surfaces at 228 K, *Geophys. Res. Lett.*, *21* (R8), 665-668, 1994.

Anderson, D.E., The troposphere to stratosphere radiation filed at twilight: A spherical model, *Planet. Space Sci.*, *31* (12), 1517-1523, 1983.

Barnes, R.J., M., Lock, J., Coleman, and A., Sinha, Observation of a New Absorption Band of HOBr and its Atmospheric Implications, *J. Phys. Chem.*, *100* (2), 453-457, 1996.

Benson, S.W., Thermochemical kinetics, 2nd ed., Wiley. New York, 1976.

Benter, Th., C., Feldmann, U., Kirchner, M., Schmidt, S., Schmidt, and R.N., Schindler, UV/VIS-absorption spectra of HOBr and CH_3OBr; Br(2P3/2) atom yields in the photolysis of HOBr, *Ber. Bunsenges. Phys. Chem.*, *99*, 1,144-1,147, 1995.

Bridier, I., Veyret, B., and R., Lesclaux, Flash photolysis kinetic study of reactions of the BrO radical with BrO and HO_2, *Chem. Phys. Lett.*, *201*, 563-568, 1993.

Burkholder, J.B., Ultraviolet absorption spectrum of HOCl, *J. Geophys. Res.*, *98*, 2,693-2,974, 1993.

Deters, B., S., Himmelmann, C. Blindauer, and J.P., Burrows, Gas phase spectra of HOBr and Br_2O and their atmospheric significance, *Ann. Geophys.*, *14* (4), 468-475, 1996.

Garcia, R., and S., Solomon, A new numerical-model of the middle atmosphere: 2-Ozone and related species, *J. Geophys. Res.*, *99* (D6), 12,937-12,951, 1994.

Glukhovtsev, M.N., A., Pross, and L., Radom, Acidities, proton affinities, and other thermochemical properties of hypohalous acids HOX (X = F-I): High-Level Computional Study, *J. Phys. Chem.*, *100* (9), 3,498-3,503, 1996.

Hanson, D.R., and A.R., Ravishankara, Heterogeneous chemistry of bromine species in sulfuric acid under stratospheric conditions, *Geophys. Res. Lett.*, *22*, 385-388, 1995.

Lary, D.J., and J.A., Pyle, Diffuse radiation, twilight and photochemistry - I, *J. Atmos. Chem.*, *13*, 373-392, 1991a, *13*, 393-406, 1991b.

Lary, D.J., M.P., Chipperfield, and R., Toumi, The potential impact of the reaction OH + ClO $\longrightarrow$ HCl + O_2 on polar ozone photochemistry, *J. Atmos. Chem.*, *21*, 61-79, 1995.

Lary, D.J., M.P., Chipperfield, R., Toumi, and T.M., Lenton, Atmospheric heterogeneous bromine chemistry, *J. Geophys. Res.*, *101* (D1), 1,489-1,504, 1996.

Logan, J.A., Trends in the vertical distribution of ozone: An analysis of ozonesonde data, *J. Geophys. Res.*, *99* (D12), 22,553-25,585, 1994.

Lock, M., R.J., Barnes, and A., Sinha, Near-threshold photodissociation dynamics of HOBr: Determination of product state distribution, vector correlation, and heat of formation, *J. Phys. Chem.*, *100*, 7,972-7,980, 1996.

McGrath, M.P., and F.S., Rowland, Ideal Gas thermodynamic properties of HOBr, *J. Phys. Chem.*, *98*, 4,773-4,775, 1994.

Meier, R.R., D.E., Anderson, and M., Nicolet, The radiation field in the troposphere and stratosphere from 240 nm to 1000 nm: General Analysis, *Planet. Space Sci.*, *30* (9), 923-933, 1982.

Nesbitt, F.L., P.S., Monks, W.A., Payne, L.J., Stirf, and R., Toumi, The reaction of $O(^3P)$ + HOBr: Temperature dependence of the rate constant and importance of the reaction as an HOBr loss process, *Geophys. Res. Lett.*, *22*, 827-830, 1995.

Nicolet, M., R.R., Meier, and D.E., Anderson, The radiation field in the troposphere and stratosphere from 240 nm to 1000 nm: Numerical Analysis, *Planet. Space Sci.*, *30* (9), 935-983, 1982.

Orlando, J.J., and J.B., Burkholder, Gas Phase UV/visible absorption spectra of HOBr and Br_2O, *J. Phys. Chem.*, *99*, 1,143-1,150, 1995.

Poulet, G., M., Pirre, F., Maguin, R., Ramaroson, and G., Le Bras, Role of the BrO + HO_2 reaction in the stratospheric chemistry of bromine, *Geophys. Res. Lett.*, *19*, 2,305-2,308, 1992.

Rattigan, O.V., O., Wild, R.L., Jones, and R.A., Cox, Temperature dependent absorption cross-sections of CF_3COCl, CF_3COF, CH_3COF, CCl_3CHO and CF_3COOH, *J. Photochem. Photobiol.* A:Chem, *73*, 1-9, 1993.

Rattigan, O.V., R.L., Jones, and R.A., Cox, The visible spectrum of gaseous OBrO, *Chem. Phys. Lett.*, *230*, 121-126, 1994.

Ruscic, B., and J., Berkowitz, Experimental determination of ΔH_f°(HOBr) and ionization potentials (HOBr): Implications for corresponding properties of HOI, *J. Chem. Phys.*, *101* (9), 7795-7803, 1994.

Salawitch, R.J., et al., The diurnal-variation of hydrogen, nitrogen and chlorine radicals - Implications for the heterogeneous production of HNO_2, *Geophys. Res. Lett.*, *21* (23), 2,551-2,554, 1994.

Seery, D.J., and D., Britton, The continuous absorption spectra of chlorine, bromine, bromine chloride, iodine chloride and iodine bromide, *J. Phys. Chem.*, *68*, 2,263-2,266, 1964.

Solomon, S., R. W. Portmann, R. R. Garcia, L. W. Thomason, L. R. Poole and M. P. McCormick, The role of aerosol variations in anthropogenic ozone depletion at northern midlatitudes, *J. Geophys. Res.*, *101* (D3), 6,713-6,727, 1996.

Thorn, R.P., Jr., P.S., Monks, L.J., Steif, S.-C., Kuo, Z., Zhang, and R.B., Klemm, Photoionization Efficiency Spectrum, Ionization Energy, and Heat of Formation of Br_2O, *J. Phys. Chem.*, *100*, 12,199-12,203, 1996.

World Meteorological Organisation, Rep. *25*, Scientific assessment of stratospheric ozone: 1991, WMO Global Ozone Research and Monitoring Project, Geneva, 1992.

Yung, Y.L., J.P., Pinto, R.T., Watson, and S.P., Sander, Atmospheric bromine and ozone perturbations in the lower stratosphere, *J. Atmos. Sci.*, *37*, 339-353, 1980.

Zintl, E., and G. Rienäcker, Über die Existenz eines flüchtigen Bromoxyds, *Ber.*, *63*, 1,098-1,104, 1930.

R.A. Cox, R.L. Jones, and D.J. Lary, Centre For Atmospheric Science, Department of Chemistry, University of Cambridge, Lensfield Road, Cambridge, CB2 1EW, England. (email: rac26@cam.ac.uk, rlj1001@cus.cam.ac.uk, david@atm.ch.cam.ac.uk)

O.V. Rattigan, Department of Chemistry, Boston College, Chestnut Hill, Boston, MA 02167, USA. (email: rattigao@bc.edu)

(Received August 8, 1995; revised May 25, 1996; accepted June 19, 1996.)